The Study on Performance of MEMS IMU for Launch Vehicle under High Vibration Environment

By Eri Shimane,[1)] Shuichi Matsumoto, [1)] Takafumi Moriguchi, [2)] Yuzo Iwai,[2)] and Ryohei Uchino [2)]

[1)] *Japan Aerospace Exploration Agency, Tsukuba, Japan*
[2)] *Sumitomo Precision Products Co., Ltd., Amagasaki, Japan*

Accuracy of MEMS gyroscope and MEMS accelerometer has been improving in recent years and JAXA has been studying a navigation grade Inertial Measurement Unit (IMU) using MEMS gyroscope and MEMS accelerometer for launch vehicles. One of issues for applying MEMS IMU for launch vehicles is to maintain measurement accuracy under high vibration environment during launch phase. Thus we developed a trial model of high accuracy MEMS IMU and evaluated the measurement accuracy of the MEMS IMU under high vibration environment by random vibration test. This paper presents the issues of MEMS IMU for launch vehicles, the trial model of MEMS IMU, and evaluation results of the MEMS IMU under high vibration environment.

Key Words: MEMS, IMU, GYRO, NAVIGATION, ROCKET

Nomenclature

ωm	:	measured angular rate in minor cycle
ωM	:	averaged angular rate in major cycle
am	:	measured acceleration in minor cycle
aM	:	averaged acceleration in major cycle
θ	:	integrated angle
v	:	integrated velocity
Rb	:	rate bias
$Rbcorr$	:	corrected rate bias
Ab	:	acceleration bias
$Abcorr$	:	corrected acceleration bias
δRb , δAb	:	preclusive rate and acceleration bias error caused by vibration machine excitation
n_{minor}	:	number of minor cycles in major cycle
N_{init}	:	number of major cycles using in initial bias estimation
N_{dif}	:	number of major cycles using bias estimation at each major cycle
T_{major}	:	duration time of major cycle
ts_{nobib} , tf_{nobib}	:	start and end time to estimate preclusive bias error caused by vibration machine excitation

Subscripts

i	:	in i-th minor cycle
j, k	:	in j-th and k-th major cycle
$init$	:	in initial bias estimation

1. Introduction

Inertial measurement unit (IMU) installed gyroscopes and accelerometers is one of most important components for guidance, navigation and control system of launch vehicles. The inertial sensors to get the information about angular rate and acceleration of launch vehicles require high accuracy, high reliability, and environment resistance. That is why existing IMUs for launch vehicles are large in size and costly.

On the other hand, gyroscopes and accelerometers for commercial use such as car navigations, controllers of video games, and smartphones become more and more small in size and low cost. Gyroscopes and accelerometer using micro electronic mechanical systems (MEMS) technology are used for these needs. MEMS devices can be mass produced with low cost, which is due to using the same production process with semiconductor. Also the accuracy of MEMS gyroscope and MEMS accelerometer has been improving in recent years.

Therefore, we have been studying to improve accuracy of MEMS gyroscope and to apply IMU using MEMS inertial sensors, which we called as MEMS IMU, for launch vehicles.

We also developed a trial model of MEMS IMU and evaluated performances of the MEMS IMU for flight condition of launch vehicles such as high vibration environment and radiation environment.

2. Issues of Applying MEMS IMU for Launch Vehicles

Since launch vehicles fly in special environment such as high vibration, wide temperature range and severe radiation environment, it is necessary for launch vehicle's IMU to resist such severe environment and to maintain high accuracy of inertial measurements. The technical issues for launch vehicle's IMU are as follows:

(1) High accuracy of inertial measurements for launch vehicle's guidance
(2) To maintain the accuracy for wide temperature range
(3) To maintain the accuracy for high vibration environment
(4) To keep normal operation for severe radiation environment

By recent improvement of MEMS IMU performances, MEMS IMU is about to be available for launch guidance of small rockets with short mission time. The second issue of the accuracy for wide temperature range can be solve by

temperature correction technique as shown in section 3. The third issue of the accuracy for high vibration is severe because MEMS gyroscope and MEMS accelerometer have mechanical structure and an antivibration mount cannot be used for inertial measurement. Thus we evaluated the accuracy deterioration of MEMS IMU under high vibration environment by random vibration test. The fourth issue of the radiation environment is another severe problem to be solve for MEMS IMU to be used for launch vehicles, which is under studying. Thus this paper concentrates the issue of maintaining the accuracy for high vibration environment.

3. Trial Model of High Accuracy MEMS IMU

To solve the issue of high accuracy inertial measurements for launch vehicle's guidance on MEMS IMU, we have developed the high accuracy MEMS angular rate sensor called MARS. [1), 2)] The high accuracy of MARS is achieved by digital temperature correction, and the latest model of MARS, MARS III, achieved low bias instability of 0.1 deg/h. [3)] Figure 1 shows the Allan variance of MARS III breadboard model with full temperature range. This result is similar to the Fiber Optical Gyroscopes (FOG) in performance, and we evaluated that the MEMS gyroscope have potentially high accuracy enough to guide and navigate launch vehicles.

As a next step, we developed a trial model of MEMS IMU to evaluate accuracy and environment resistance in the configuration of IMU. The model number of the MEMS IMU trial model is HGM-02A whose appearance and specifications are shown in Fig. 2 and Table 1. One of main issues of MEMS IMU for flight conditions of launch vehicles is high vibration environment. To see whether resist and maintain its performance in the vibration environment of H-IIA rocket, we conducted random vibration test using the MEMS IMU trial model.

Fig. 2. Trial model of MEMS IMU (HGM-02A)

Table 1. Specifications of MEMS IMU (HGM-02A).

Items	Specifications
Size	74(W)×74(L)×60(H) [mm]
Weight	500 [g]
Angle rate measurement range	±100 deg/s
Angle rate measurement accuracy	1 deg/s rms
Angle rate measurement resolution	0.001 deg/s
Acceleration measurement range	±2 G
Acceleration measurement accuracy	0.2 G rms
Acceleration measurement resolution	0.1 mG

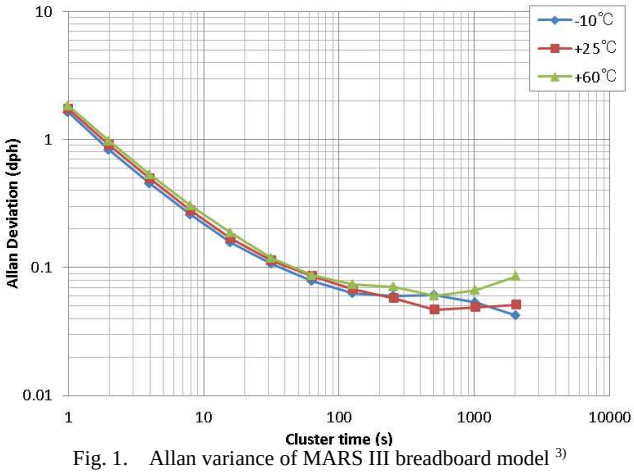

Fig. 1. Allan variance of MARS III breadboard model [3)]

4. Vibration Test Results and Data Analyses

4.1. Vibration test setup and conditions

To evaluate angular rate and acceleration measurement accuracy of MEMS IMU in high vibration environment, we carried out vibration test using the trial model of MEMS IMU, HGM-02A, at Tsukuba Space Center in February 2017. Figure 3 shows the picture of vibration test setup. Since this vibration test was carried out as a part of the vibration test campaign for commercial-off-the-shelf (COTS) navigation sensors, COTS global navigation satellite system (GNSS) modules were tested with the MEMS IMU. The MEMS IMU was set on the center of vibration test table shown as in Fig. 3. Although many test patterns and vibration levels were conducted in this vibration test campaign, we used the random vibration level profile for H-IIA onboard components as a reference in this paper. The random vibration level profile is shown in Fig. 4 and its overall acceleration root-mean-square (RMS) is 79 m/s^2 (rms) . In this paper, vibration test results of z-axis vibration, which is perpendicular to the vibration test table, are shown and discussed.

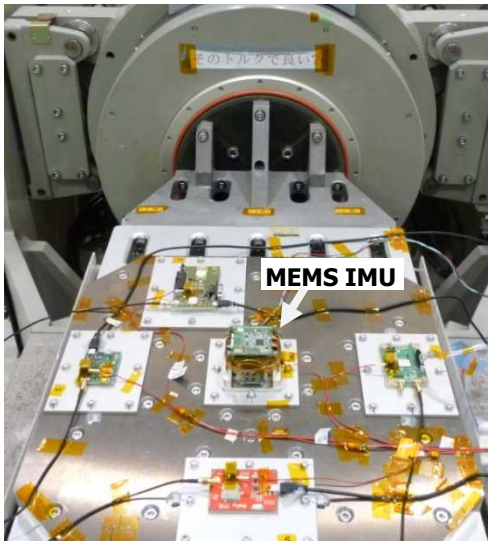

Fig. 3. Vibration test setup

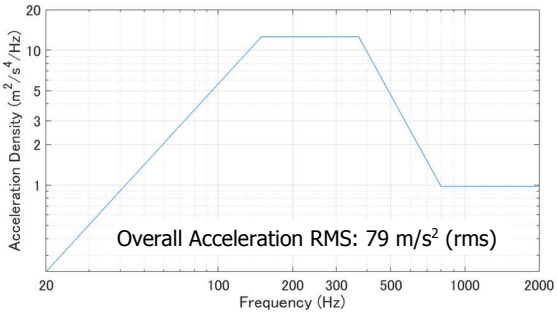

Fig. 4. Random vibration level profile for H-IIA onboard components

4.2 Data acquisition results of vibration tests

In the vibration test, angular rate and acceleration measurements of the MEMS IMU were obtained with a sampling rate of 50 Hz. Figure 5 shows one of the vibration test results using H-IIA vibration level profile shown in Fig. 4. About 50 seconds before vibration start, vibration machine table was excited by electromagnetic force for vibration motion, which is indicated as a symbol, '△' , in Fig. 5. Vibration motion starts from a level of -24 dB of target vibration lever and its vibration level is increased step by step with 6 dB until target vibration level. Since Fig. 5 is test results of z-axis vibration, the increase of vibration level can be seen in the z-axis acceleration data in Fig. 5, which is the bottom of right-hand side in Fig. 5. The vibration start time is indicated as a symbol, '▲' , and the duration of target vibration level is indicated as a symbol, '◆' , in Fig. 5.

From Fig. 5, we can recognize that the measurement data sampled at 50 Hz are very noisy and it is difficult to evaluate small bias errors of high accuracy MEMS IMU from raw measurement data.

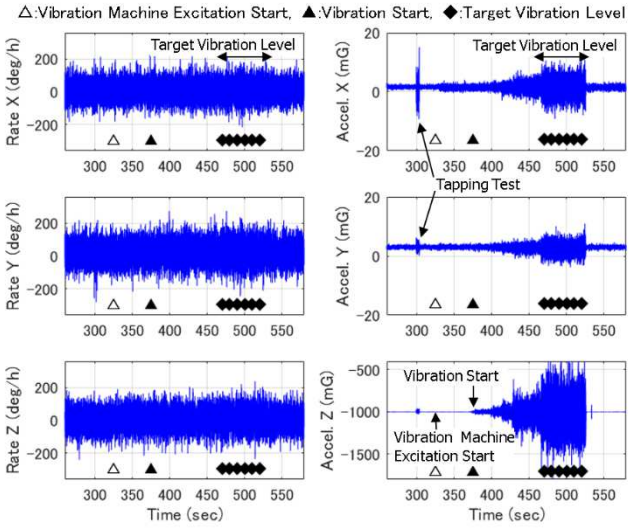

Fig. 5 Angular rate and acceleration raw measurement data of the MEMS IMU (sampling rete is 50 Hz)

4.3 Data analysis methods and results of vibration tests

To evaluate small bias errors on high accuracy MEMS IMU, noise on raw measurement data has to be reduced. Averaging technique is used to reduce noise on the data, and in addition to that, data integration technique is employed to extract small bias errors. In this paper, we call raw measurement data of 50 Hz sampling as minor cycle data, and the averaged data of the measurement data for 1 second as major cycle data, which means minor cycle is 50 Hz and major cycle is 1 Hz. Averaged angular rate, 'ωM', and averaged acceleration, 'aM', are obtained as Eqs. (1) and (2).

$$\omega M_j = \frac{1}{n_{minor}} \sum_{i=1}^{n_{minor}} \omega m_{ji} \tag{1}$$

$$aM_j = \frac{1}{n_{minor}} \sum_{i=1}^{n_{minor}} am_{ji} \tag{2}$$

Although the averaging is very useful for reducing noise on measured data, it is not enough to extract small bias error on high performance MEMS IMU. Thus as a next step we employ data integration technique for each single axis. Integrated angle, 'θ' , and integrated velocity, 'v' , are defined as Eqs. (3) and (5). Since MEMS gyroscopes and MEMS accelerometer have initial bias errors, which are to be canceled by initial alignment operation, the integrated angles and accelerations are integrated after subtracting initial bias errors as in Eqs. (3) and (5). The initial bias errors are estimated by averaging more than 100 seconds before vibration operation start as shown in Eqs. (4) and (6). The number of major cycles using in initial bias estimation, 'N_{init}' , is more than 100.

$$\theta_k = T_{major} \cdot \sum_{j=1}^{k} (\omega M_j - Rb_{init}) \tag{3}$$

$$Rb_{init} = \frac{1}{N_{init}} \sum_{j=1}^{N_{init}} \omega M_j \tag{4}$$

$$v_k = T_{major} \cdot \sum_{j=1}^{k} (aM_j - Ab_{init}) \tag{5}$$

$$Ab_{init} = \frac{1}{N_{init}} \sum_{j=1}^{N_{init}} aM_j \tag{6}$$

The integrated angles and velocities corresponding to the measured data in Fig. 5 are shown in Fig. 6. The small slops starting from the initial flat zero in Fig. 6 are caused by small bias error on angular rates and accelerations of MEMS IMU. From Fig. 6 we can recognize small bias errors on integrated angles of all axes and integrated velocities of x and y axes and relatively large bias error on integrated velocity of z axis. Also we can find that the small bias errors arise not from vibration start but from vibration machine excitation start.

To quantize the bias errors during vibration motion, averaged bias errors are calculated using the time difference of integrated angles and velocities as shown in Eqs. (7) and (8). N_{dif} in Eqs. (7) and (8) is the number of major cycle using bias estimation at each major cycle and is set to 10,. which means averaging time is 10 seconds, in this paper.

$$Rb_k = \frac{\theta_k - \theta_{k-N_{dif}}}{N_{dif} \cdot T_{major}} \quad (7)$$

$$Ab_k = \frac{v_k - v_{k-N_{dif}}}{N_{dif} \cdot T_{major}} \quad (8)$$

The estimated angular rate biases and acceleration biases corresponding to the measured data in Fig. 5 are shown in Fig. 7. From Fig. 7 we can recognize clearly small bias errors on integrated angles of all axes and integrated velocities of x and y axes and relatively large bias error on integrated velocity of z axis. We also find that the small bias errors arise not from vibration start but from vibration machine excitation start. We assume that this small bias errors after vibration machine excitation start are due to electromagnetic sensitivity of MEMS IMU and the electromagnetic radiation from the vibration machine excited by electromagnetic force for vibration motion. Separately from this paper, we will confirm the cause of this bias errors after vibration machine excitation start and in this paper, this bias errors after vibration machine excitation start are treated as the bias errors to be excluded for the accuracy evaluation of the MEMS IMU under high vibration environment.

To estimate preclusive bias errors after vibration machine excitation start, we extracted the period when the vibration machine was excited and vibration motion was not started. The preclusive bias errors after vibration machine excitation start is estimated by averaging bias errors during the extracted period as shown in Eqs. (10) and (12). And angular rate bias errors and acceleration bias errors caused by vibration motion are estimated by subtracting the preclusive bias error as shown in Eqs. (9) and (11).

$$Rbcorr_k = Rb_k - \delta Rb \quad (9)$$

$$\delta Rb = \frac{\theta_{tf_{novib}} - \theta_{ts_{novib}}}{tf_{novib} - ts_{novib}} \quad (10)$$

$$Abcorr_k = Ab_k - \delta Ab \quad (11)$$

$$\delta Ab = \frac{v_{tf_{novib}} - v_{ts_{novib}}}{tf_{novib} - ts_{novib}} \quad (12)$$

4.4 Angular rate bias errors caused by vibration motion

Same data analyses discussed in section 4.3 were done for all valid z-axis vibration test data using the H-IIA vibration level profile and its level-down profiles. Estimated angular bias errors caused by vibration motion are shown in Fig. 8. H-IIA vibration level whose overall acceleration RMS is 79 m/s^2 (rms) is corresponding to '0 dB' in Fig. 8. From Fig. 8, we can recognize that the angular rate bias errors caused by random vibration motion are proportional to vibration level, i.e. acceleration spectral density. Using the estimated angular rate bias errors of z axis shown in Fig. 8, vibration rectification error (VRE) is estimated as about 0.5 deg/h/G_{rms}.

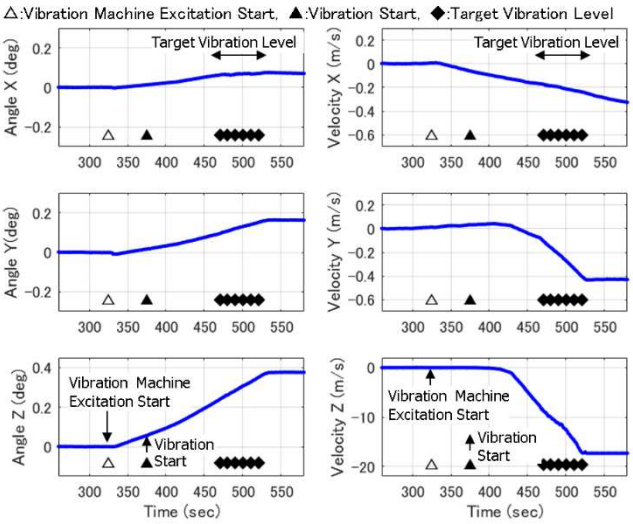

Fig. 6 Integrated angles and velocities of the MEMS IMU corresponding to the measured data in Fig. 5

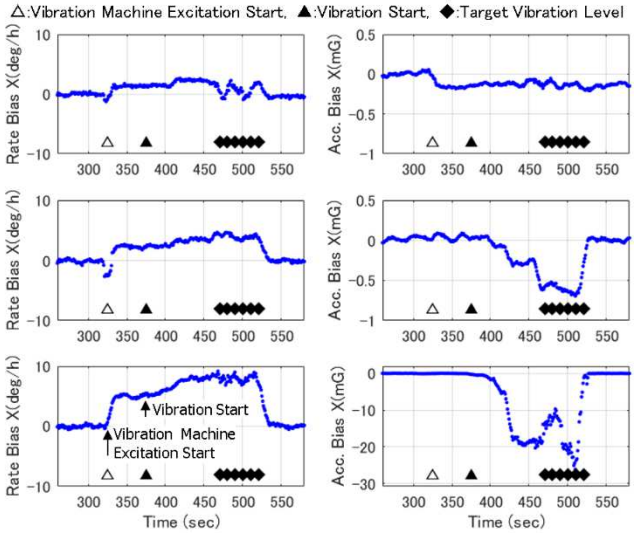

Fig. 7 Estimated angular rate biases and acceleration biases corresponding to the measured data in Fig. 5

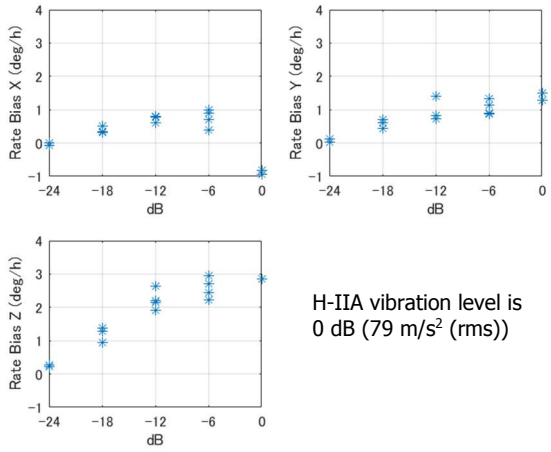

Fig. 8 Estimated angular rate bias error caused by vibration motion

5 Accuracy Evaluation under High Vibration Environment

5.1 Angular rate accuracy evaluation under high vibration

As shown in the z-axis vibration test data evaluation results discussed in section 4.4, the maximum angular rate bias error caused by the H-IIA level vibration is about 3 deg/h, which is larger than that of H-IIA IMU. However we think the MEMS gyroscope of the MEMS IMU trial model can be apply to a small rocket whose mission time is short and orbital insertion accuracy is not so severe and to a onboard flight path monitoring system for rocket flight safety using with global positioning system (GPS) receiver.

5.2 Acceleration accuracy evaluation under high vibration

As shown in the right-hand side bottom plot in Fig. 7, the z axis acceleration bias is very large and we think it is difficult to use the acceleration outputs of the MEMS IMU trial model under high vibration environment as inertial measurements for launch vehicle's navigation. We figured out the root cause of the large z-axis bias error as resonance between MEMS accelerometer and printed wiring board (PWB). Since MEMS accelerometers are attached directory on a PWB, MEMS accelerometer resonated with PWB at the natural frequency of the PWB. To cope with this problem, we made the design change that MEMS accelerometers are installed on a sensor mount.

6. Conclusion

We have tested the MEMS IMU trial model in the vibration environment of H-IIA vibration level. From the vibration test and its data evaluation, we extracted technical issues to be solve on MEMS IMU system design and recognized the accuracy of MEMS IMU under high vibration environment. We think that the design of the MEMS IMU trial model, HGM-02A, and modified MEMS accelerometer mount design can be apply to a small rocket whose mission time is short and orbital insertion accuracy is not so severe. We will continue to study about accuracy and environment resistance of MEMS IMU to apply MEMS IMU for launch vehicles.

References

1) Sasada, T., Shimane, E., Nishida, H., Moriguchi, T., Uchino, R., Magosaki, F.: An Interim Report on the Development of High-Accuracy MEMS Gyros for Space Applications, Proceedings of 57th Space Sciences and Technology Conference, 2G02, Yonago, 2013, (in Japanese).
2) Sasada, T., Shimane, E., Nishida, H., and Moriguchi, T.: Development of High-Accuracy MEMS Gyros for Space Applications, 9th ESA Round Table on Micro and Nano Technologies for Space Applications, Lausanne, 2014.
3) Sasada, T., and Nishida, H.: Adaptation of Navigation-grade MEMS Gyros for Future Launch System, Proceedings of 30th International Symposium on Space Technology and Science, Kobe, 2015.